

1 Supplementary Information

2

3 Supplementary Methods

4

5 Vulnerability-targeted greening scenarios

6

7 Because the proximity-based InVEST Scenario Generator allocates new tree cover preferentially near existing
8 vegetation, it cannot explicitly prioritize underserved neighborhoods or areas with high heat risk. To address
9 this limitation, we developed an additional set of targeted greening scenarios that prioritize planting locations
10 based on the joint distribution of heat exposure and social vulnerability. These scenarios represent targeted
11 alternatives to the proximity-based greening pathways and are referred to as Target10, Target20 and Target30,
12 corresponding to 10%, 20% and 30% relative increases in tree canopy cover, respectively. The targeted
13 planting workflow consisted of four steps.

14 1) Identification of candidate planting locations. We first generated candidate tree-planting points
15 along London's street network using OpenStreetMap (OSM) road data. Different road classes were treated
16 using separate spatial rules. For active transport routes, including pedestrian paths, footways and cycleways,
17 candidate points were generated directly along road centerlines at 5 m intervals. For vehicle-accessible roads,
18 specifically residential and unclassified streets, we first created parallel offset lines 3.5 m to both sides of the
19 centerline to approximate sidewalk planting space, and then generated candidate points every 5 m along these
20 offset lines.

21 2) Application of biophysical and spatial constraints. We then filtered candidate points to retain only
22 physically suitable planting locations. To reduce competition with existing canopy and ensure sufficient
23 growing space, new planting points were kept away from existing trees. We used a 1 m resolution tree canopy
24 raster and buffered existing canopy pixels by 5 m using morphological dilation; candidate points falling within
25 this buffered area were removed. To avoid conflicts with buildings, we excluded points located within 2 m of
26 building footprints. Because the road-offset procedure often produced clustered points near intersections, we
27 then applied a KD-tree nearest-neighbor filter and removed points located within 5 m of one another. This step
28 produced a more realistic and spatially uniform planting density.

29 3) Prioritization by heat exposure and social vulnerability. Remaining candidate points were ranked
30 using a composite priority score based on local heat exposure and social vulnerability. Heat exposure was
31 represented by 1 m resolution Universal Thermal Climate Index (UTCI) values at 14:00 local time, extracted for
32 each candidate point; points outside the valid simulation extent were excluded. To combine UTCI with the
33 Social Vulnerability Index (SVI), UTCI values were rescaled to a 0–1 range using min–max normalization. We
34 then assigned the tract-level SVI percentile to each candidate point using a spatial join. Because SVI percentile
35 also ranges from 0 to 1, the final priority score was calculated as $Priority\ score = UTCI_{norm} \times SVI$.
36 Candidate points were ranked in descending order of this score, such that higher-priority locations represent
37 the co-occurrence of more severe heat stress and higher social vulnerability.

38 4) Generation of targeted greening scenarios. To construct the three targeted greening scenarios, we
39 selected the highest-ranked candidate points and converted them to a 10 m × 10 m grid to match the
40 resolution of the LULC and urban cooling models, using average crown-size assumptions to represent canopy
41 extent. Candidate sites were added in rank order until each canopy expansion target was reached. For
42 Target10, approximately 565,000 tree sites were selected, corresponding to the Mayor's target of a 10%
43 relative increase in tree canopy cover by 2050. For Target20 and Target30, approximately 1,129,000 and

44 1,819,000 tree sites were selected, respectively. These totals are approximate, as some projected tree crowns
45 may overlap., using average crown-size assumptions to represent canopy extent. Together, Target10, Target20
46 and Target30 provide vulnerability-targeted alternatives to the proximity-based greening scenarios (Green10,
47 Green20 and Green30), allowing direct comparison between spatially opportunistic and explicitly equity-
48 oriented tree planting pathways.

49

50 **Estimation of future relative humidity (RH)**

51 Relative humidity (RH) is one of the key input data for Urban Cooling mode. We estimate future RH under
52 projected climate by using near-surface air temperature (T, °C) and actual vapor pressure based on the
53 WorldClim v2.1 1970–2000 monthly climatology (vapr, kPa):

$$54 \quad RH = 100 \times \frac{e_a}{e_s(T)}$$

55 The temperature-dependent saturation vapor pressure (e_s , hPa)—representing the maximum moisture-
56 holding capacity of the urban boundary layer at a given temperature—was computed using the improved
57 Tetens-form approximation ^{1,2}.

$$58 \quad e_s(T) = 6.112 \times \exp\left(\frac{17.67 \times T}{T + 243.5}\right)$$

59 where T is air temperature in degrees Celsius (°C), and T in future is estimated by using the average of
60 (Tmax + Tmin) / 2, or to simplify, T = Tx from WorldClim v2.1 CMIP6 future temperature data. e_a is actual
61 water vapor pressure in hPa, and $e_a = 10 * \text{vapr}$. This temperature-driven approach assumes constant
62 atmospheric moisture (i.e., fixed dew point or specific humidity) and may therefore overestimate drying in
63 regions where moisture increases under warming. However, it provides a transparent and internally consistent
64 first-order estimate suitable for scenario comparison ³. For a hot London month, expect higher water vapor
65 pressure—roughly ~1.5 kPa on average, with ~1.3–1.6 kPa typical on summer days.

66

67

68

69 **Supplementary Tables and Figures**

70

71 **Urban Cooling Modeling**

72

73 **Sup. Table 1 | Land use and climate scenario combinations used in urban cooling modeling.** The table shows
 74 all combinations of land use and land cover (LULC) scenarios and climate conditions evaluated in this study.
 75 Climate scenarios are defined by projected mean summer reference air temperature and urban heat island
 76 (UHI) intensity for the specified year (2021, 2050 and 2070). The temperature–UHI combinations are used to
 77 parameterize the urban cooling model (see Methods). An “x” indicates scenario combinations implemented in
 78 the modelling.

Year	2021 (Baseline)	2050	2070
LULC scenarios	Climate scenarios (Reference air temperature + UHI combinations)		
	22°C + 2°C	25°C + 5°C	28°C + 5°C
S0 – Baseline	x	x	x
S1 – AllBuilt		x	x
S2 – TreeOpp		x	x
S3 – TreeRisk		x	x
S4 – Green10		x	x
S5 – Green20		x	x
S6 – Green30		x	x
S7 – Target10		x	x
S8 – Target20		x	x
S9 – Target30		x	x

79

80

81

82 **Sup. Table 2 | Biophysical parameters used in the Urban Cooling Model (UCM).** Parameters were compiled
 83 based on a UCM calibration study ⁴, FAO crop coefficient values
 84 (<https://www.fao.org/4/x0490e/x0490e0b.htm#crop%20coefficients>), and ECOTRESS Albedo data ⁵.

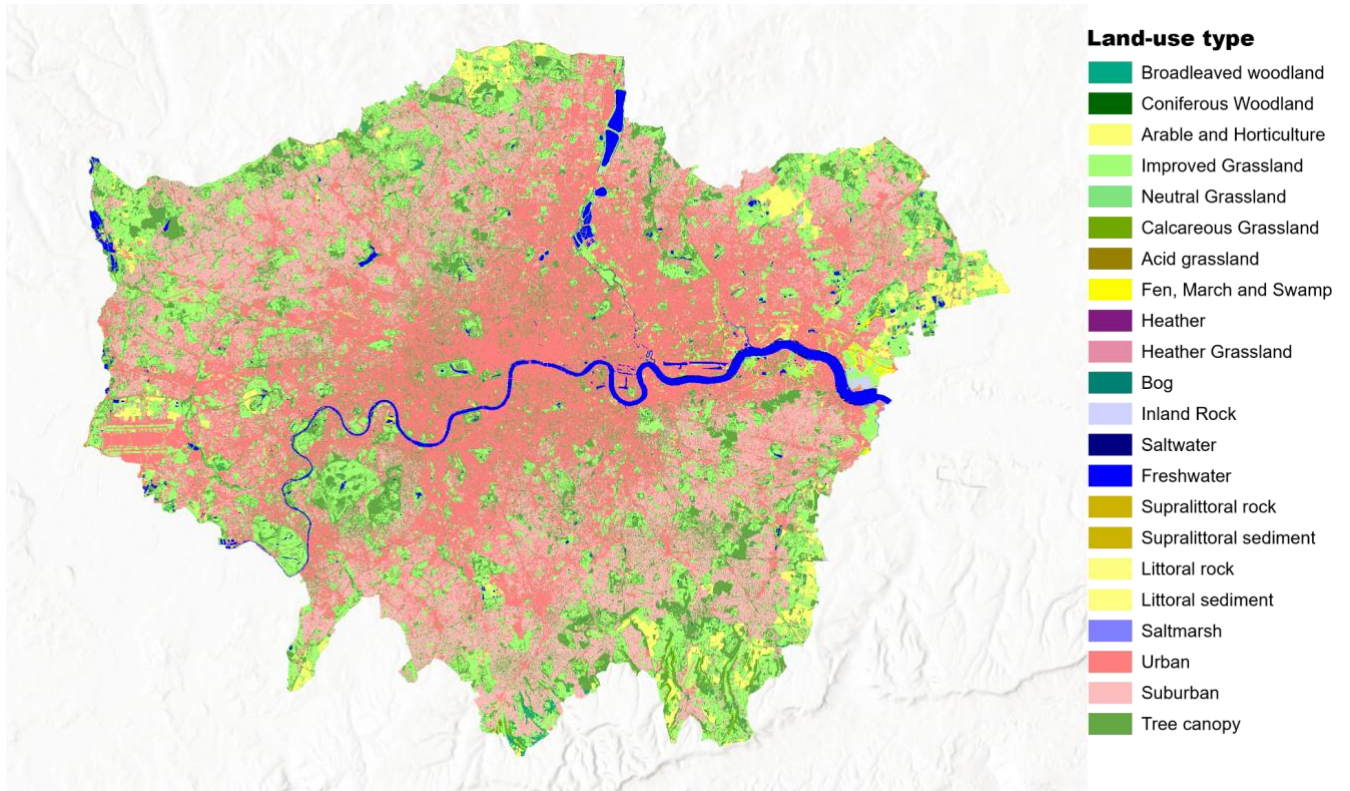
Land-use code	Description	Shade	Kc (Crop coefficient)	Albedo	Green area	Building intensity
1	Deciduous woodland	0	0.7	0.12	1	0
2	Coniferous woodland	0	0.7	0.11	1	0
3	Arable	0	0.3	0.12	0	0
4	Improved Grassland	0	0.8	0.13	1	0
5	Neutral Grassland	0	0.7	0.13	1	0
6	Calcareous Grassland	0	0.7	0.12	1	0
7	Acid grassland	0	0.7	0.12	0	0
8	Fen, Marsh, and Swamp	0	0.9	0.12	1	0
9	Heather	0	0.8	0.10	1	0
10	Heather grassland	0	0.8	0.13	1	0
11	Bog	0	0.8	0.12	1	0
12	Inland Rock	0	0.8	0.11	0	0
13	Saltwater	0	0	0.08	0	0
14	Freshwater	0	1	0.08	0	0
15	Supralittoral Rock	0	0.8	0.12	0	0
16	Supralittoral Sediment	0	0.8	0.12	0	0
17	Littoral Rock	0	0.8	0.12	0	0
18	Littoral Sediment	0	0.8	0.09	0	0
19	Saltmarsh	0	0.8	0.10	0	0
20	Urban	0	0.2	0.11	0	0.75
21	Suburban	0	0.3	0.11	0	0.5
100	Tree Cover	1	0.8	0.12	1	0
0	Nothing	0	0	0	0	0

85

86 **Sup. Table 3 | Key climate parameters used in Urban Cooling Model.** The table summarizes the climate inputs
 87 used to parameterize the Urban Cooling Model for baseline and future conditions. The year 2021 was selected
 88 as the baseline reference year, and simulations focus on July, historically the warmest month in London.
 89 Reference air temperature and urban heat island (UHI) intensity represent representative summer conditions
 90 for each time horizon. Air blending distance and maximum cooling distance were held constant across
 91 scenarios to isolate the effects of land-use change. Reference evapotranspiration (Ref ET) values were derived
 92 from CGIAR historical datasets for current conditions and from CGIAR future projections (2041–2060 and 2061–
 93 2080) under SSP370 and SSP585 for mid- and late-century scenarios. Average relative humidity reflects
 94 representative July conditions for each year.

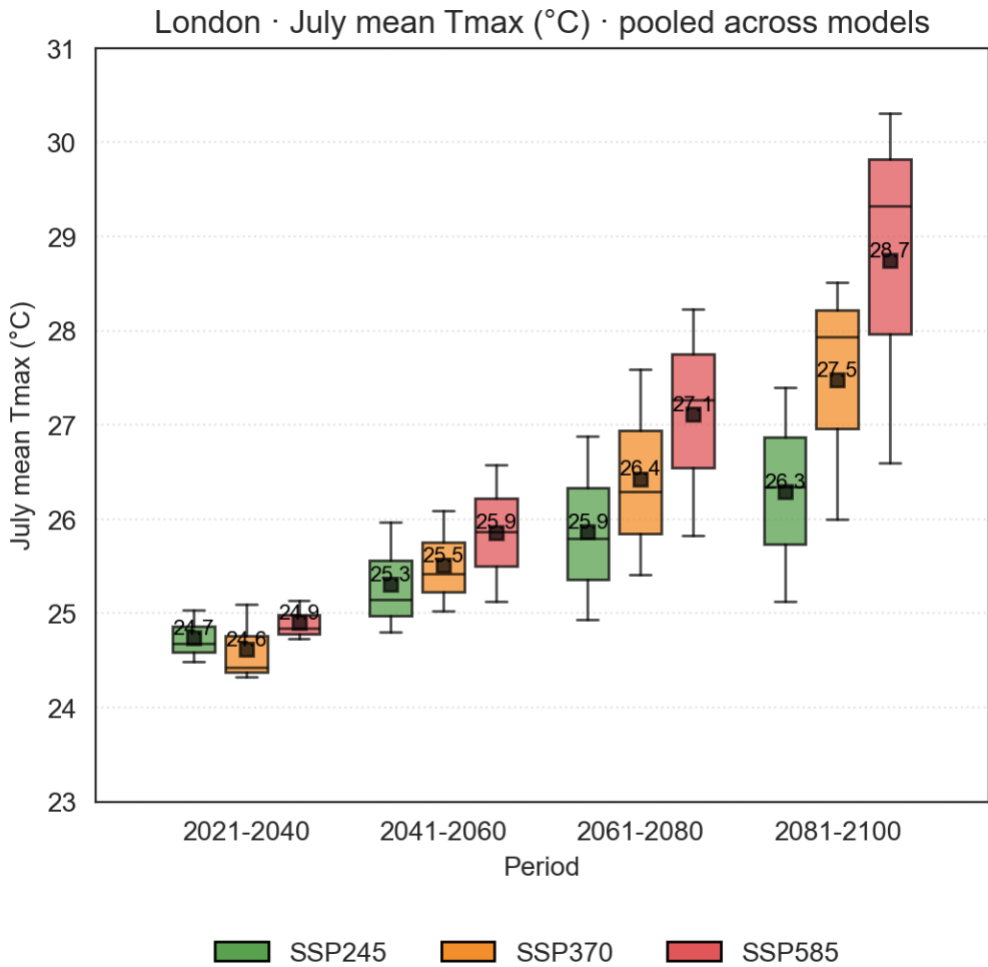
Year	Reference air temperature (°C)	UHI effect (°C)	Air Blending distance (m)	Max cooling distance (m)	Ref ET (mm)	Average Relative Humidity (%)
2021 (Baseline year)	22	2	500	450	CGIAR (1980-2000)	55
2050	25	5	500	450	CGIAR model future (2041-2060) SSP 370 or 585)	45
2070	28	5	500	450	CGIAR model future (2061-2080) SSP 370 or 585)	42

95
96



97
 98
 99
 100
 101

Sup. Fig. 1 | London land use and land cover (LULC) in 2021. This baseline LULC layer was used to parameterize the Urban Cooling Model and to generate alternative land-use scenarios (see Methods). Data source: UK Centre for Ecology & Hydrology (UKCEH).

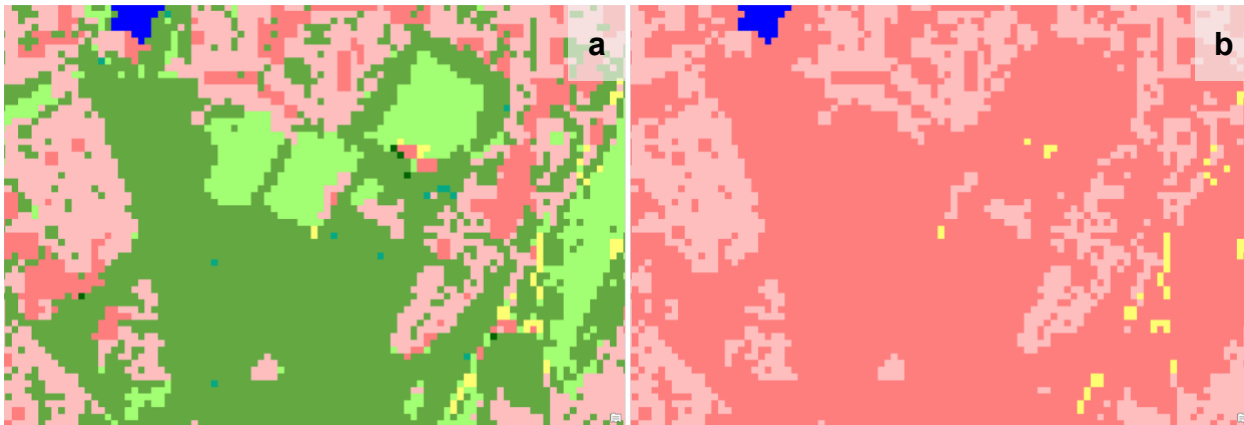


102
 103
 104
 105
 106
 107
 108
 109
 110

Sup. Fig. 2 | Projected changes in July mean maximum temperature (Tmax) in London under future climate scenarios. Box plots show model-pooled projections of July mean Tmax across four time periods under SSP245, SSP370, and SSP585. Boxes indicate the interquartile range, center lines denote the median, and whiskers represent 1.5× the interquartile range. Values are pooled across climate models (see Methods). Following common practice in climate projection studies, the periods 2021–2040, 2041–2060, 2061–2080 and 2081–2100 are used to represent conditions centered approximately on 2030, 2050, 2070 and 2090, respectively.

111 **Land use and land cover scenarios**

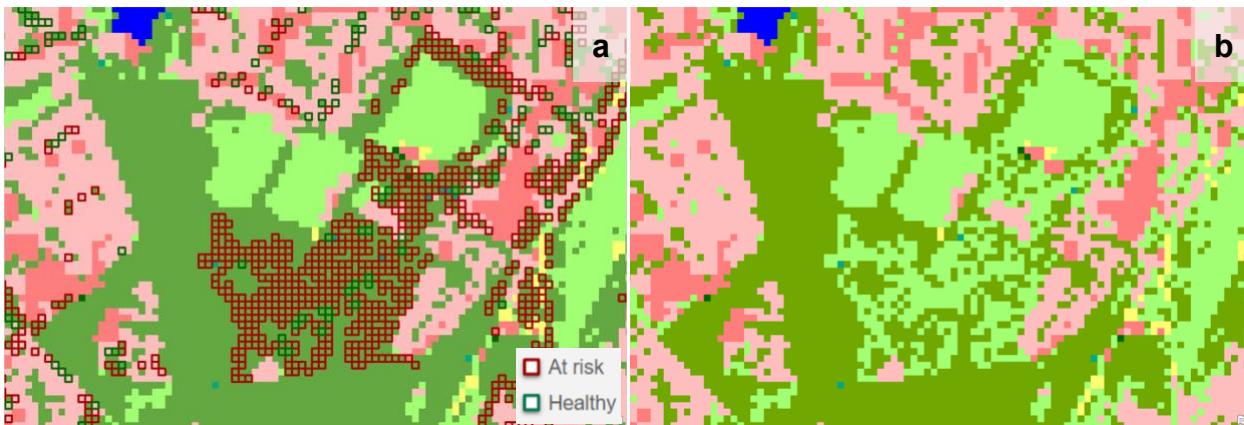
112



113

114 **Sup. Fig. 3 | Example of the vegetation-to-impervious conversion scenario.** The scenario converts all natural
115 land-cover classes, including deciduous woodland, coniferous woodland, improved grassland, neutral
116 grassland, calcareous grassland, acid grassland and heather grassland, to urban built-up land. a, Baseline LULC
117 map. b, LULC scenario map after vegetation-to-impervious conversion. The LULC categories and color scheme
118 are the same as in Sup. Fig. 2.

119

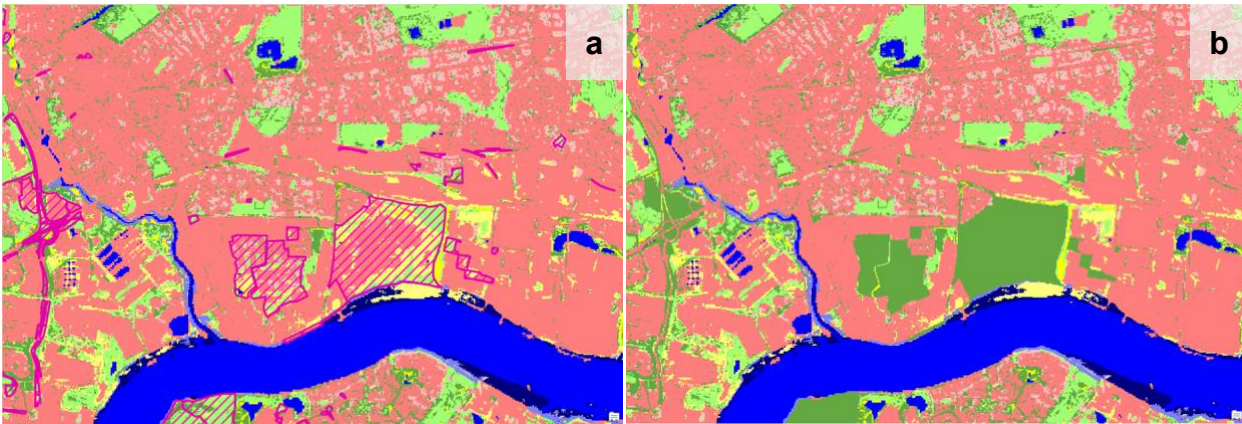


120

121 **Sup. Fig. 4 | Example of the climate-driven tree canopy loss scenario.** Areas in red squares denote individual
122 trees will be at climate risk, and pixels within green squares represent individual trees would remain healthy
123 under future climate change scenarios (a). Trees at future climate risks would degrade and be converted to
124 grassland (b). The LULC categories and color scheme are the same as in Sup. Fig. 2.

125

126



127
 128 **Sup. Fig. 5 | Example of the opportunity tree planting scenario.** Increasing tree cover by converting
 129 opportunity land (primarily unused areas) to tree cover. Left (a): baseline LULC map (areas with magenta
 130 diagonal hatching indicate potential opportunity land for greening); right (b): scenario map. The LULC
 131 categories and color scheme are the same as in Sup. Fig. 2.

132
 133



134
 135 **Sup. Fig. 6 | Examples of the Policy target (+10% canopy), ambitious greening (+20% canopy), and**
 136 **transformative greening (+30% canopy) scenarios.** The LULC categories and color scheme are the same as in
 137 Sup. Fig. 2.

138 **Energy saving associated with urban cooling**

139

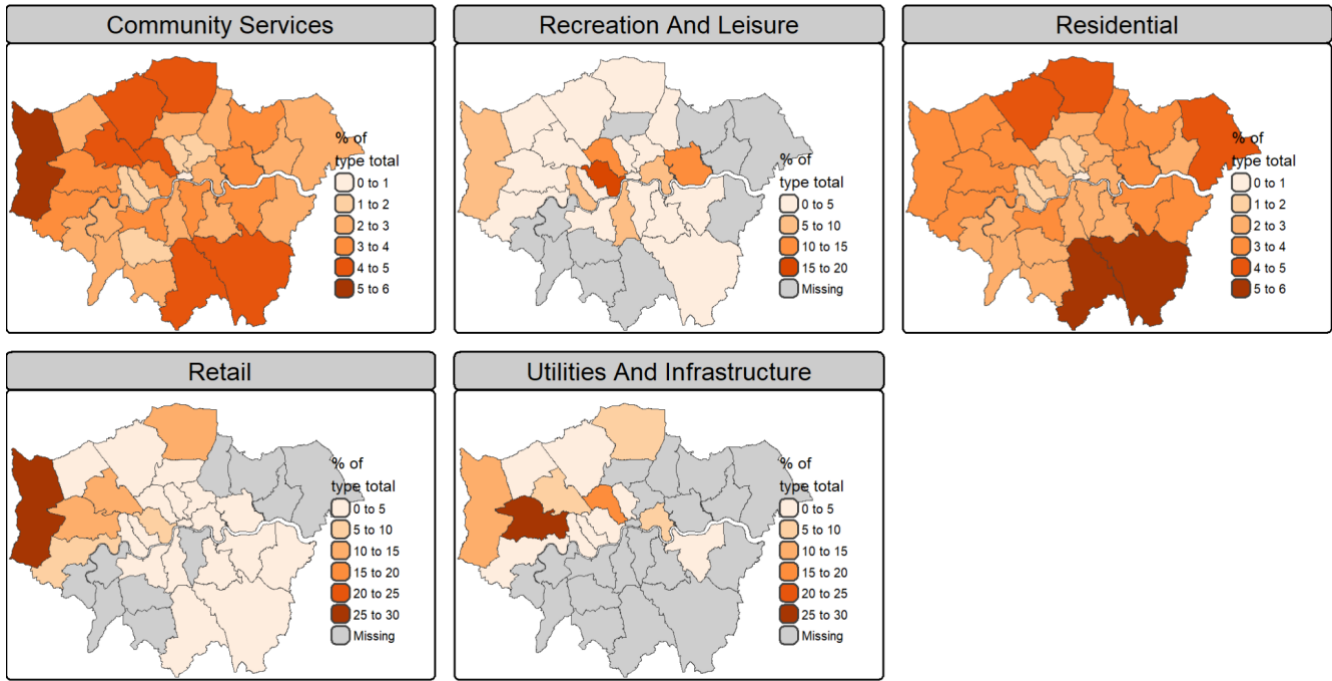
140 **Sup. Table 4 | Energy consumption parameters by building types in London.**

Building Type ID	Building type name	Building category	Consumption (kWh /m ² / °C) per month *	Cost (£ per kWh)	Area (m ²) **
-1	NA	Other	0.00	0.0000	9,837,414
0	Agriculture And Fisheries	Industry	0.00	0.2700	25,083
1	Community Services	Services - Leisure and community	9.89	0.2800	12,238,412
2	Defense	Services - Defense / Military	0.00	0.2700	21,617
3	Industry and Business	Industry	0.00	0.2550	3,186,094
4	Minerals	Industry	0.00	0.2700	58
5	Mixed Use	Services - Commercial	0.00	0.2800	2,180,096
6	Recreation And Leisure	Services - Leisure and community	9.89	0.2800	806,529
7	Residential	Domestic - Residential	0.01	0.2563	221,990,513
8	Retail	Services - Retail	30.80	0.2700	1,538,350
9	Transport	Transport	0.00	0.2700	2,264,476
10	Unclassified, presumed non-residential	Other	0.00	0.2700	4,382,640
11	Utilities And Infrastructure	Services - Commercial	19.19	0.2800	183,840
12	Vacant And Derelict	Other	0.00	0.2700	66,633

141 * Energy consumption was estimated from https://www.drax.com/wp-content/uploads/2018/08/180809_Drax_Q2_Report.pdf

142 ** Building area is calculated from the building footprint data (see Methods)

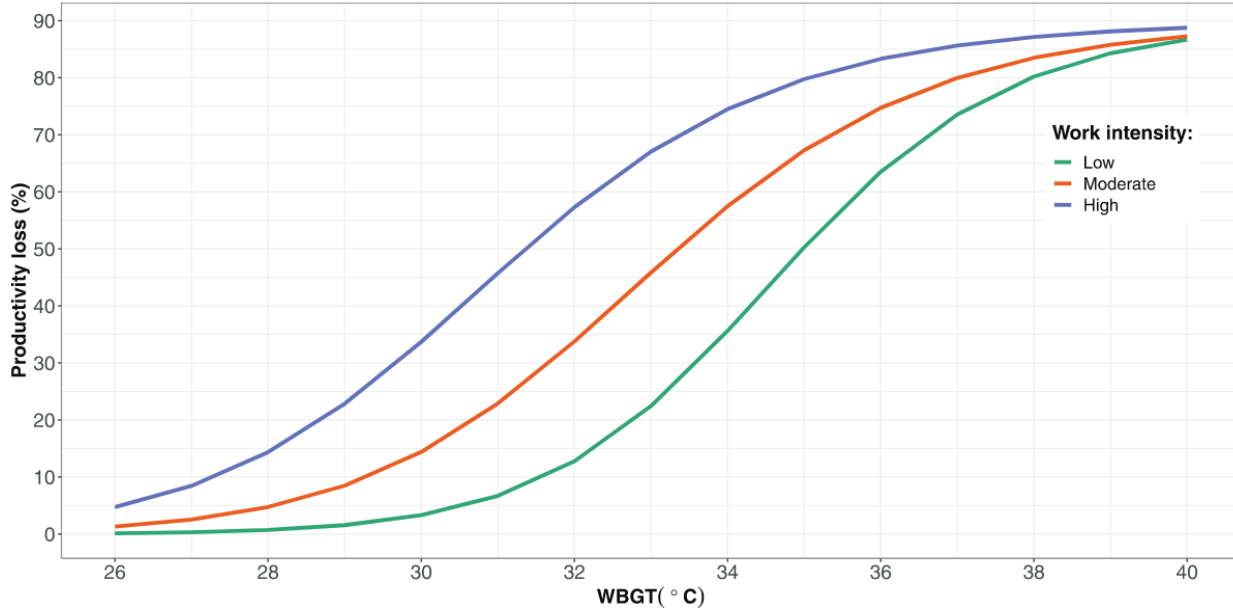
143



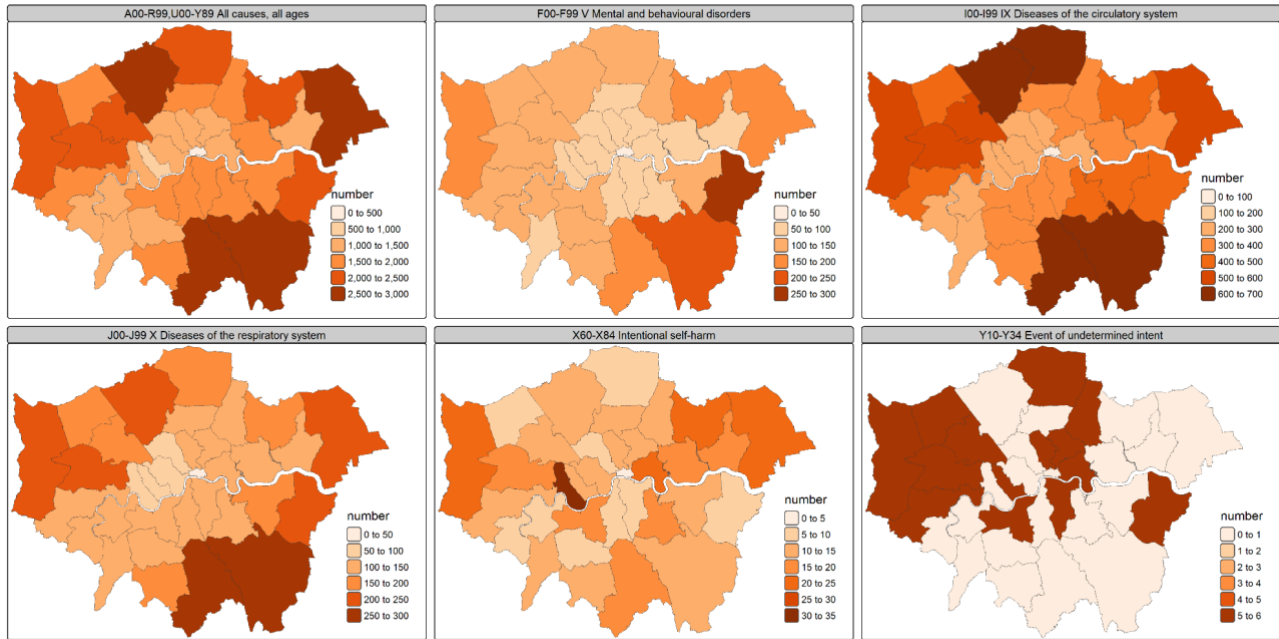
144
 145
 146
 147
 148
 149

Sup. Fig. 7 | Spatial distribution of building types across London. Maps show, for each borough, the share of citywide building area (%) for five broad building-type categories (refer to Sup. Table 4 for the classification). Grey shading denotes boroughs with missing or unavailable data.

150 **Work productivity**



151 **Sup. Fig. 8 | Exposure-response functions describing the relationships between heat (measured by wet-bulb**
 152 **globe temperature, WBGT) and productivity loss. The figure was adapted from Orlov et al ⁶.**
 153

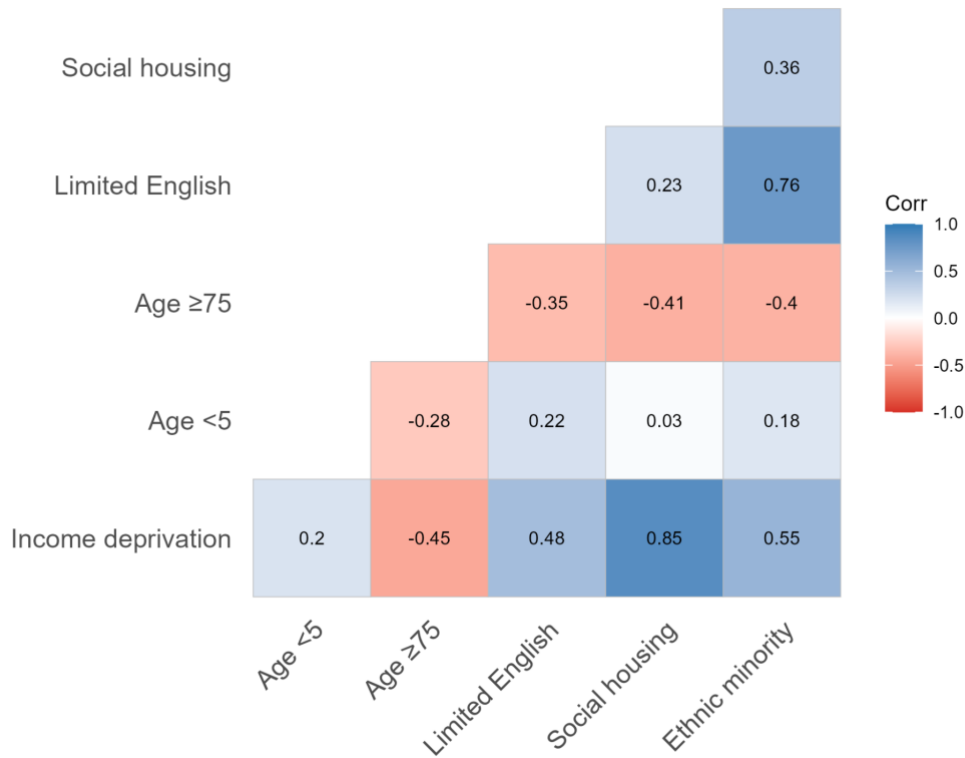


154 **Sup. Fig. 9 | Baseline cause-specific mortality rates in 2021. The maps show baseline mortality rates in London**
 155 **for 2021 across selected ICD-10 categories: (1) all causes (A00–R99, U00–Y89; all ages), (2) mental and**
 156 **behavioral disorders (F00–F99), (3) diseases of the circulatory system (I00–I99), (4) diseases of the respiratory**
 157 **system (J00–J99), and (5) intentional self-harm (X60–X84). These baseline rates were used to parameterize**
 158 **health impact estimates under alternative land-use and climate scenarios.**
 159

160

161 **Social vulnerability index**

162



163

164 **Sup. Fig. 10 | Correlations among neighborhood vulnerability metrics in London.** Heatmap shows pairwise
165 Pearson correlation coefficients between six sociodemographic vulnerability indicators at the Lower Layer Super
166 Output Area (LSOA) level. Colors indicate the direction and magnitude of correlations (blue, positive; red,
167 negative), and values are shown within each cell. Metrics include income deprivation, children aged <5, older
168 adults aged ≥75, limited English proficiency, social housing, and ethnic minority population. Strong positive
169 correlations indicate that several vulnerability dimensions co-occur spatially across London, whereas negative
170 correlations reflect trade-offs in neighborhood age structure relative to socioeconomic and demographic
171 vulnerability.

172

a



b



173
174
175
176

Sup. Fig. 11 | Social vulnerability index by LSOA (a) and by borough (b) in London.

177 **Supplementary References**

- 178 1. Bolton, D. The Computation of Equivalent Potential Temperature.
- 179 <https://journals.ametsoc.org/view/journals/mwre/108/7/1520->
- 180 [0493_1980_108_1046_tcocept_2_0_co_2.xml](https://journals.ametsoc.org/view/journals/mwre/108/7/1520-0493_1980_108_1046_tcocept_2_0_co_2.xml) (1980).
- 181 2. Yuan, W. *et al.* Increased atmospheric vapor pressure deficit reduces global vegetation growth. *Science*
- 182 *Advances* **5**, eaax1396 (2019).
- 183 3. Lawrence, M. G. The Relationship between Relative Humidity and the Dewpoint Temperature in Moist Air: A
- 184 Simple Conversion and Applications. <https://doi.org/10.1175/BAMS-86-2-225> (2005) doi:10.1175/BAMS-86-
- 185 2-225.
- 186 4. Hamel, P. *et al.* Calibrating and validating the Integrated Valuation of Ecosystem Services and Tradeoffs
- 187 (InVEST) urban cooling model: case studies in France and the United States. *Geoscientific Model*
- 188 *Development* **17**, 4755–4771 (2024).
- 189 5. Hook, S., Halverson, G., Johnson, M. & Cawse-Nicholson, K. ECOSTRESS Tiled Ancillary NDVI and Albedo L2
- 190 Global 70 m v002. https://doi.org/https://doi.org/10.5067/ECOSTRESS/ECO_L2T_STARS.002 (2023).
- 191 6. Orlov, A., Sillmann, J., Aunan, K., Kjellstrom, T. & Aaheim, A. Economic costs of heat-induced reductions in
- 192 worker productivity due to global warming. *Global Environmental Change* **63**, 102087 (2020).
- 193